NOT FOR DISTRIBUTION

011764-509-M

11764-509-M = RL-2247

30 October 1973

MEMO TO: File

FROM: E. F. Knott

SUBJECT: Cross Section Reduction by Means of Resistive Sheets

I. Introduction

This memorandum describes the results of a series of numerical experiments whose purpose was to determine the effectiveness of resistive sheets in reducing non-specular scattering. The study was motivated by two facts: a) a computer program already existed which solves the two-dimensional integral equation for metallic cylinders in the presence of such sheets and b) resistive sheets are physical realities and are available for several discrete values of resistivity. The computer program is one step closer to reality than the one used previously (based on an impedance boundary condition) because a physical property of a real substance is explicitly embedded in the integral equations.

The body chosen as a test obstacle was a metallic ogival cylinder 3λ wide and two versions of a computer program were used in the study. The programs are based on integral equations (4.47) and (4.48) of Knott and Senior (1973) and are named REST and RISK. Program REST is itself a modified version of program RAMC furnished to us by AFAL and a listing of REST is given in Knott, Liepa and Senior (1973). Program RISK is essentially a copy of REST except that it prints out the phase of the scattering in addition to the amplitude, and it also prints out the scattering from individual segments of the body profile as well as the total. We found this feature to be highly useful in decomposing the scattering into its components, but only after program REST had been run for several cases. Using RISK, we have succeeded in resolving the resistive

sheet scattering into components arising from the leading and trailing edges of the sheet and we can now explain the source of strange "resonances" observed earlier, both at the Radiation Laboratory and at Teledyne Ryan Aeronautical Corporation. Moreover, because of this resolution, we have established an absolute limit on the radar cross section reduction available by the use of a single resistive sheet.

II. Preliminary tests

Initially two configurations of resistive sheets were studied, one using a single flat sheet placed in the plane of symmetry and attached to the ogival cylinder, and the other being a cap made of two curved sheets and stationed $\lambda/4$ ahead of the cylinder. These configurations are sketched in Fig. 1. In

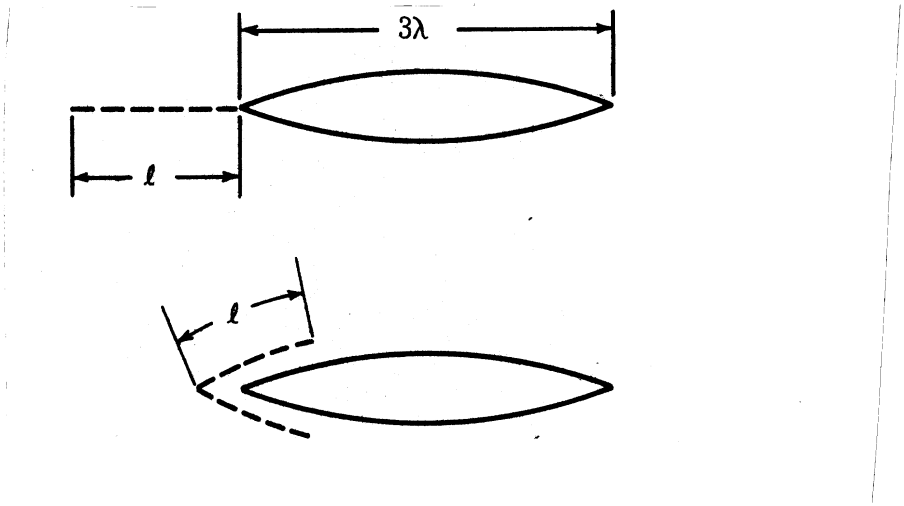

FIG. 1: Resistive sheet configurations

both cases the cylinder was 3λ wide and the width ℓ of the sheets was varied from 0.25λ to 1λ. Both linear and parabolic (square law) resistance variations were studied, always with a high, but adjustable resistance at the leading edge

of the sheet and tapering toward zero at its trailing edge. Although we later permitted the leading edge resistance (R_{max}) to be as large as 4.0 (normalized with respect to 377 ohms), it was held to a value of 2.0 or less in these preliminary studies.

Typical edge-on cross sections of the two configurations are shown in Fig. 2 for sheets 0.75λ wide. The single flat sheet outperforms the curved double sheet configuration by 5 dB or better, and in both cases the linear variation proves to be better than the parabolic. This is not necessarily true for all sheet widths, however; other data (not shown) for the double sheet have nulls that are deeper than those for a single sheet (to be presented in a moment), but we now know that these nulls are due to the interference between the leading and trailing edges of the sheet and are thus highly vulnerable to small changes in frequency. Since the single sheet performs better than the two-sheet configuration, we focussed on it for most of the study.

III. A flat sheet with three different distributions

The effects of sheet width and maximum leading edge resistance are shown in the cross section data in Figs. 3 to 6 for linear, parabolic and cubic resistance distributions, respectively. These cross sections are for edge-on incidence only, but for the most part the reductions persist out to 30 or 40 degrees from edge-on. A cursory comparison of the three figures quickly shows that the cross sections tend to converge toward the dashed line ("resistive half-plane") for the parabolic and cubic distributions as the sheet grows wider, but that no such convergence is apparent for the linear distribution. A careful inspection of Fig. 3 reveals that sheet widths an odd multiple of $\lambda/4$ produce much deeper nulls than those which are an odd multiple of $\lambda/2$. These nulls shift to the right as the sheet width increases, hence they occur at progressively higher values of R_{max}. This "resonance" phenomenon has also been observed

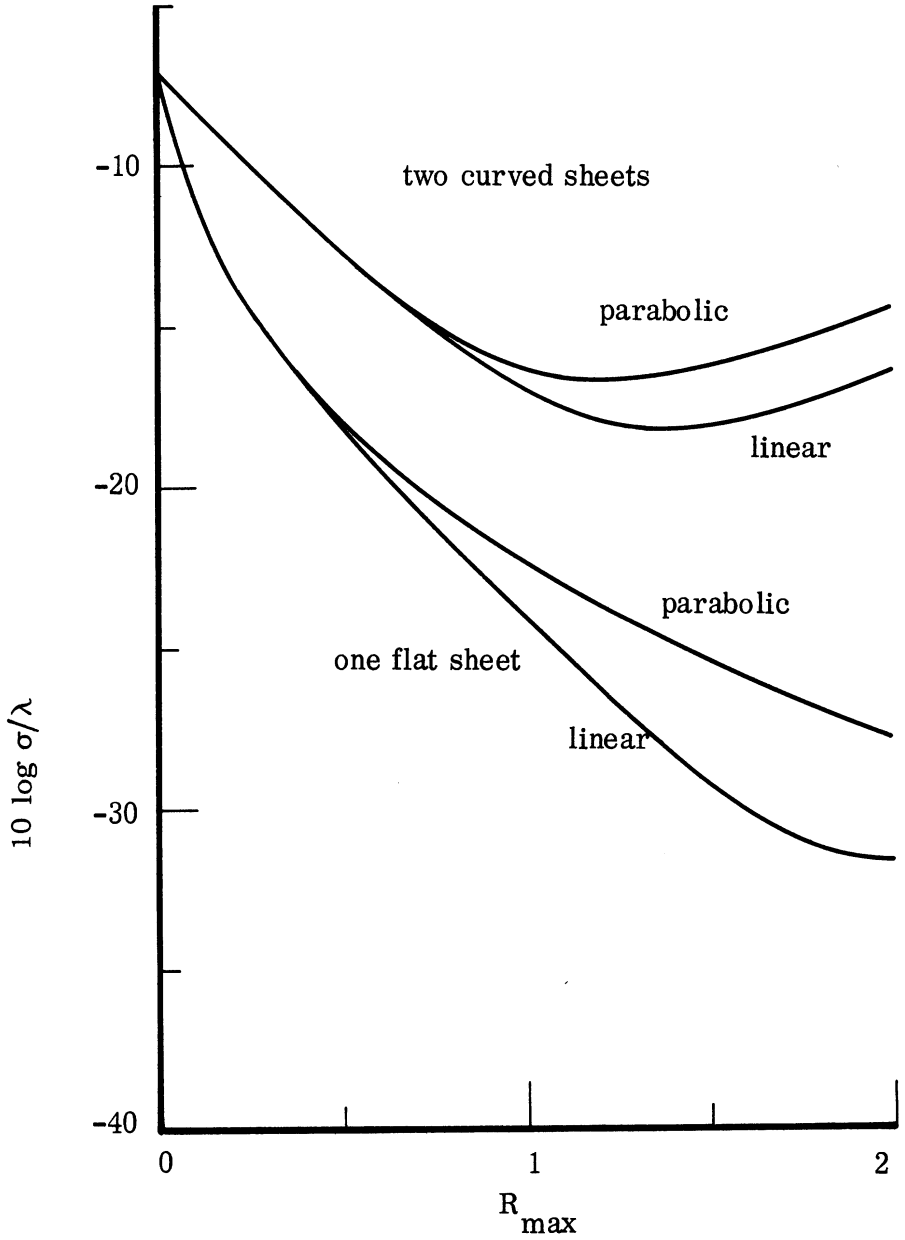

FIG. 2: A single flat sheet performs better than two curved sheets. The sheets were 0.75λ wide.

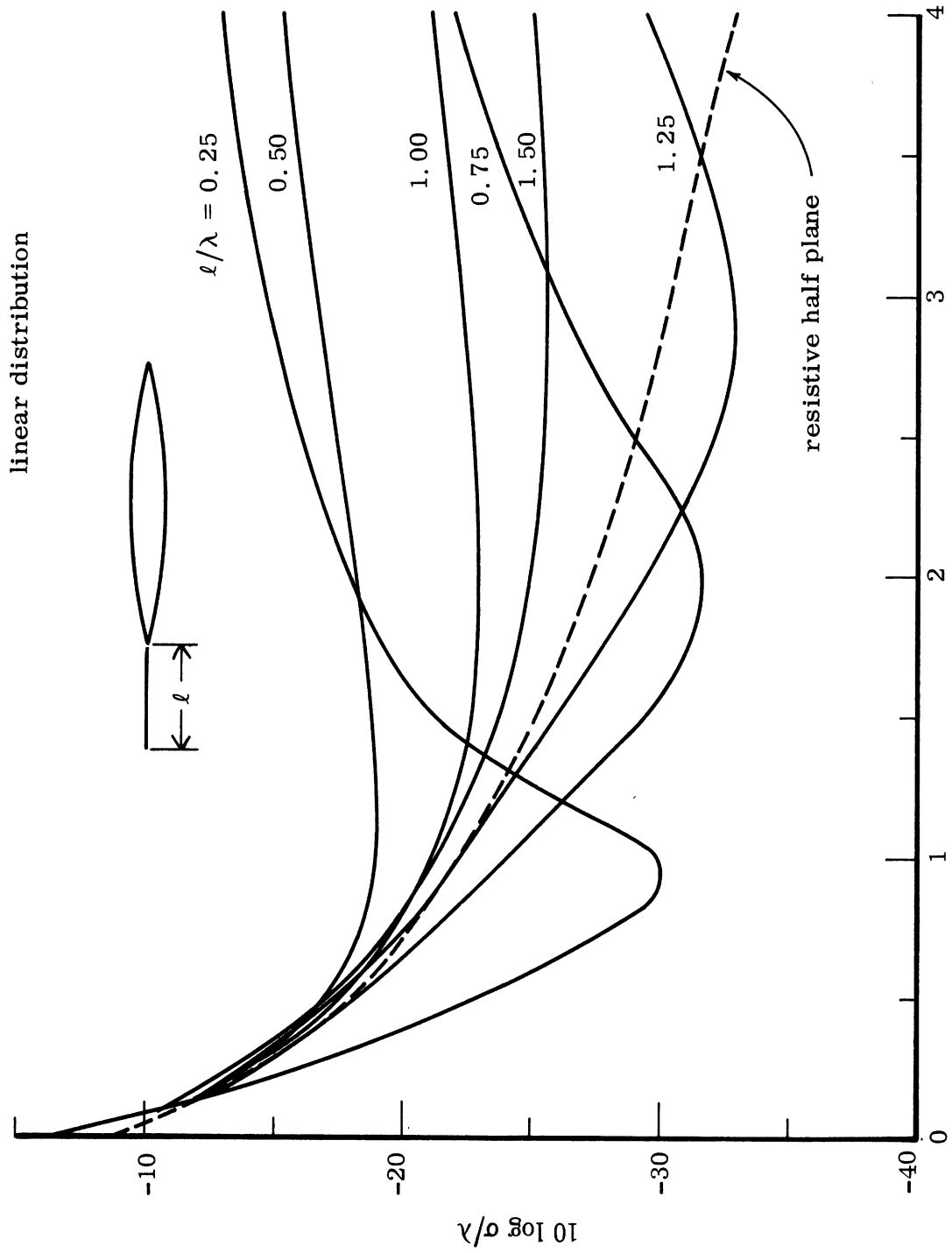

FIG. 3: Edge-on scattering from cylinder-sheet combination for linear resistance distribution.

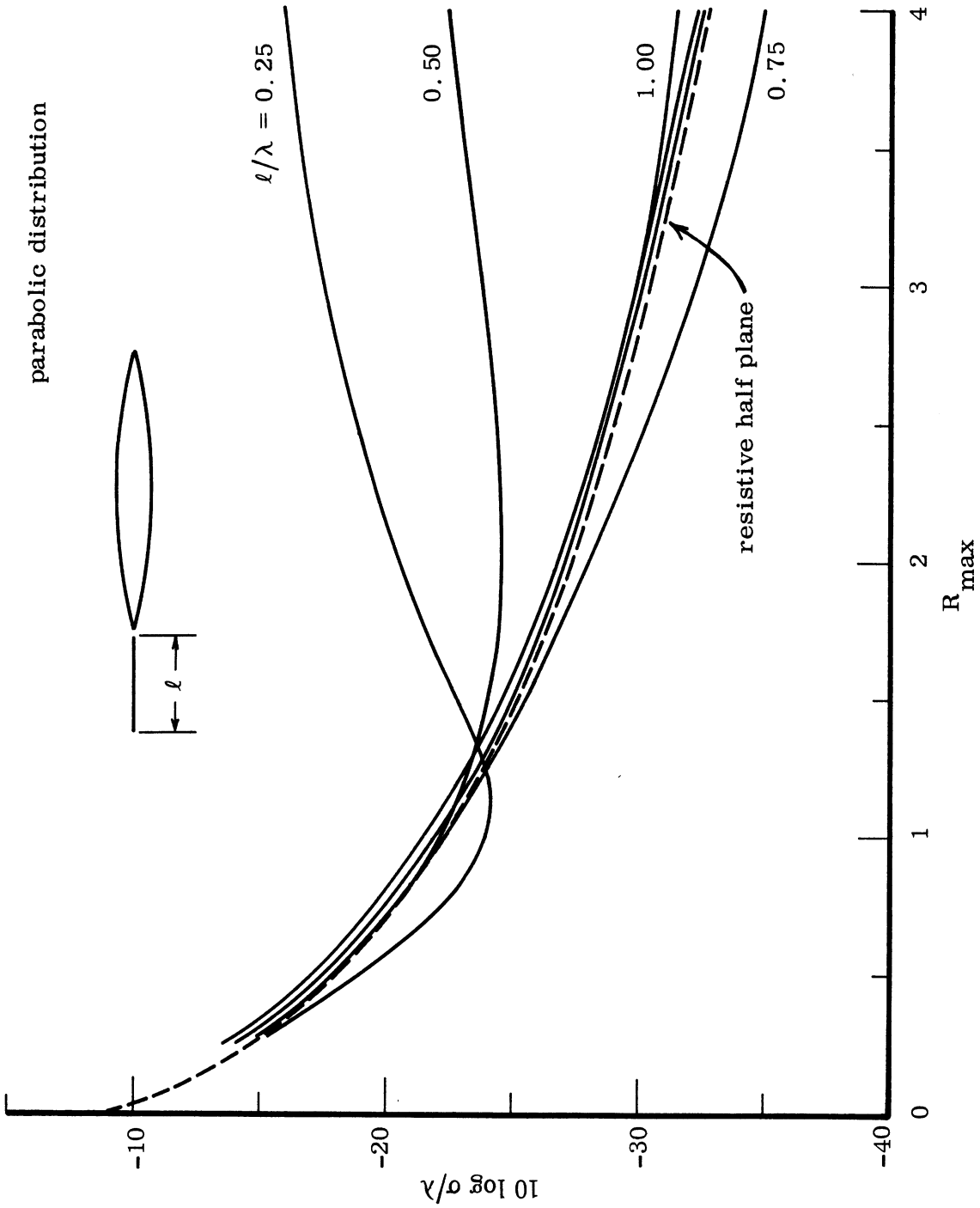

FIG. 4: Edge-on scattering from cylinder-sheet combination for parabolic resistance distribution.

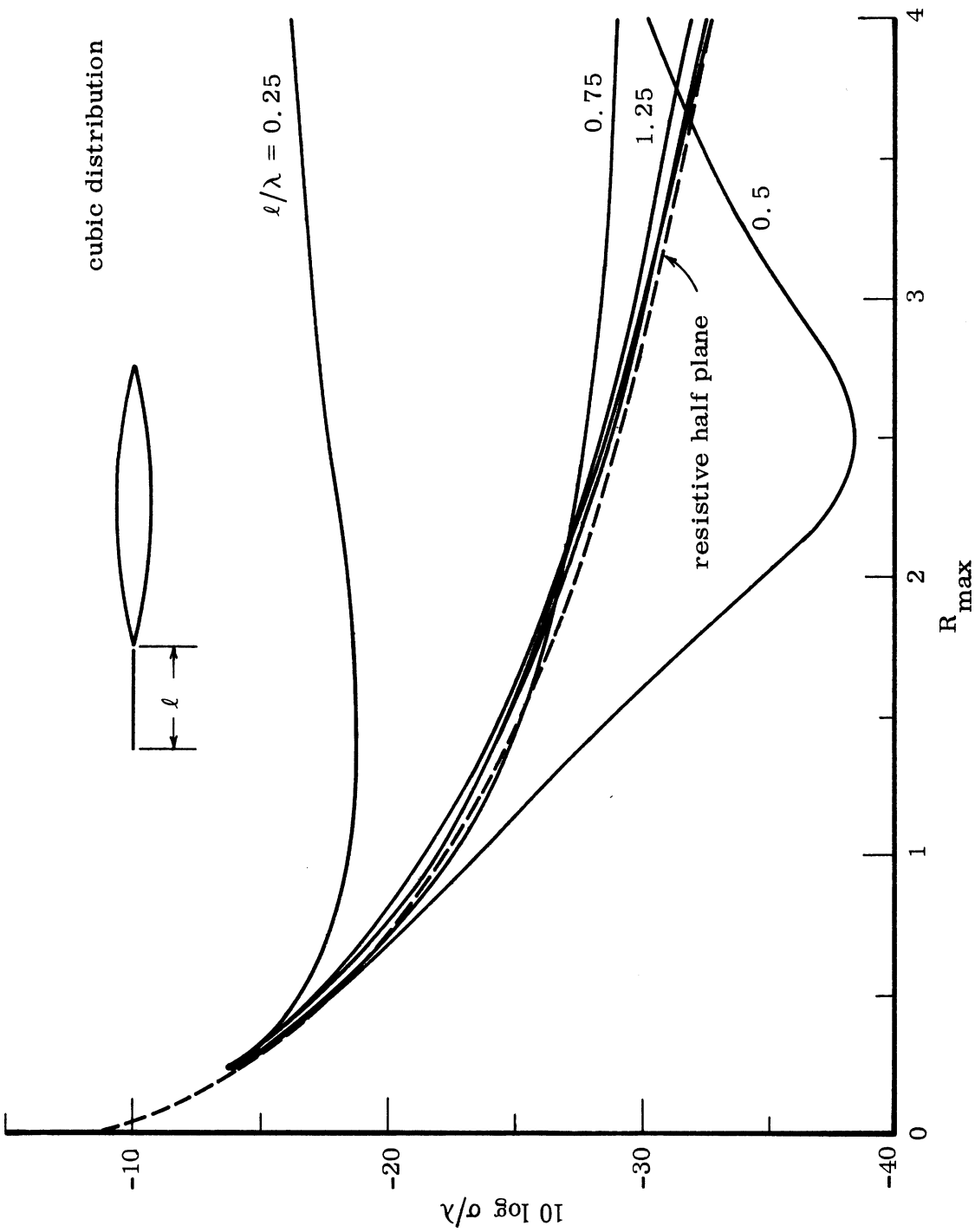

FIG. 5: Edge-on scattering from cylinder-sheet combination for cubic resistance distribution.

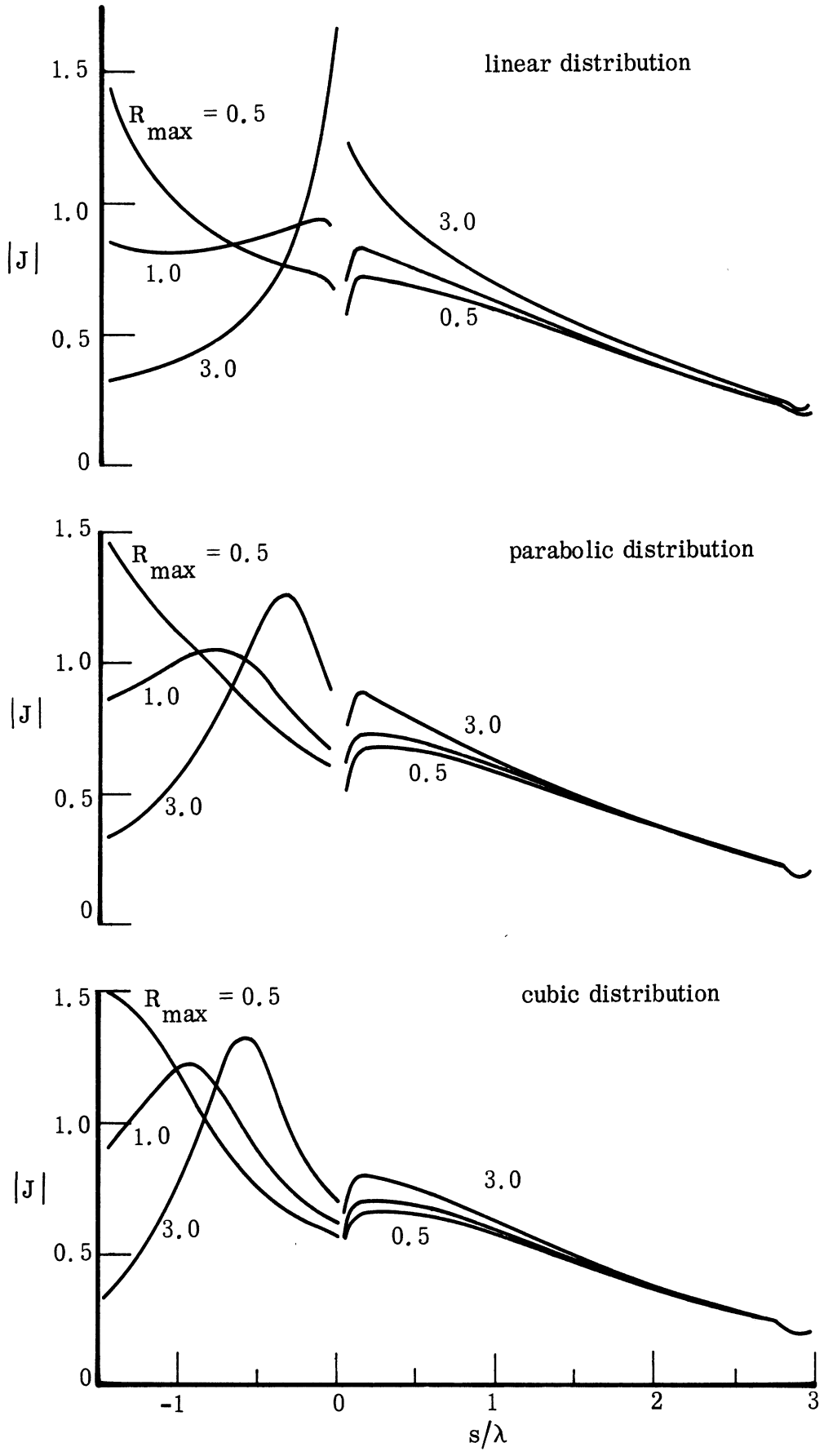

FIG. 6: Surface current distribution over sheet-cylinder combination for three resistance variations.

by Teledyne Ryan Aeronautical Corporation in its resistive sheet studies. Except for the narrowest of the sheets (0.25λ and 0.50λ), the parabolic and cubic distributions display none of the resonances seen in the linear case.

A selection of surface current distributions for the three kinds of resistance variations is plotted in Fig. 6 for a sheet 1.5λ wide. The curves on the left side of the diagram represent the resistive sheet currents while those on the right side represent the currents on the metallic cylinder. Since the far field scattering is in essence the sum of all currents, and since the currents are the same on opposite sides of the body for edge-on incidence, we have doubled the bare body values for one side of the body so as to provide a more representative amplitude scale for comparing the currents on the two kinds of surface. The phase of the currents increases from the front of the ensemble to the rear at very nearly the same rate as that of the incident wave, but due to perturbations, the phase at some locations can deviate as much as 90 degrees from that of the incident wave.

Note that the currents at the leading edge of the sheet are virtually independent of the resistance variation, being about 1.5, 0.9 and 0.35 for values of R_{max} of 0.5, 1.0 and 3.0, respectively. (Similarly, the current intensity at the trailing edge of the metallic cylinder is quite independent of the presence of the sheet.) For small values of R_{max}, the current decays at approximately the same rate away from the leading edge of the sheet independently of the type of resistance distribution, although the initial decay is slightly more rapid for a linear distribution than for a cubic. For large values of R_{max}, the current builds up from the front toward the rear instead of decaying and, depending upon the particular distribution imposed, may attain a peak value before reaching the rear edge. The location of this current peak shifts toward the leading edge of the sheet as the order of the distribution increases from linear through cubic.

Although the far field scattering shown in Figs. 3 through 5 is obtained via the integration of the surface current distributions like those shown in Fig. 6, it is not immediately apparent how the differences between the linear and parabolic

far field scattering can be deduced from the surface fields. In our previous work with H-polarization, the surface fields usually had oscillatory patterns due to surface waves travelling in opposite directions, and the amplitudes of the interfering components could be deduced. However, there are no such oscillations for the E-polarized currents and such a decomposition cannot be easily performed on the basis of the surface field data alone.

IV. Isolated sheets

Puzzled by the differences in the results for linear and higher order distributions, we collected comparable sets of data for an isolated sheet. The hope was, of course, that the isolated sheet, being a less complicated obstacle, would lead to an understanding of the scattering mechanism involved. The back-scattering results for linear and parabolic distributions are plotted in Figs. 7 and 8 and it is immediately apparent that the cross section of an isolated sheet is higher than that of a cylinder-sheet configuration. The resonant effect is still present for a linear distribution, although to a lesser degree, as is revealed in Fig. 7, and the curves still tend to converge on the dashed line for the parabolic distribution as seen in Fig. 8, although at a much slower rate than observed for the cylinder-sheet configuration.

A selection of surface field distributions on the isolated sheets is given in Fig. 9, and note that the distance scale has been expanded from that of Fig. 6. In general the fields behave similarly to those for which the conducting cylinder is present; in particular, the amplitudes of the currents at the leading edge of the sheet seem to be independent of the presence of the conducting cylinder and as R_{max} increases, the peak in the current distribution shifts from the front of the sheet toward the rear. However, in contrast to the current distributions on the cylinder-sheet combination, those on the isolated sheet exhibit small but distinct oscillations. Presumably these are due to surface waves arising from scattering from the trailing edge of the sheet and their very presence implies that the return from the rear edge of the sheet is larger in the absence of the cylinder

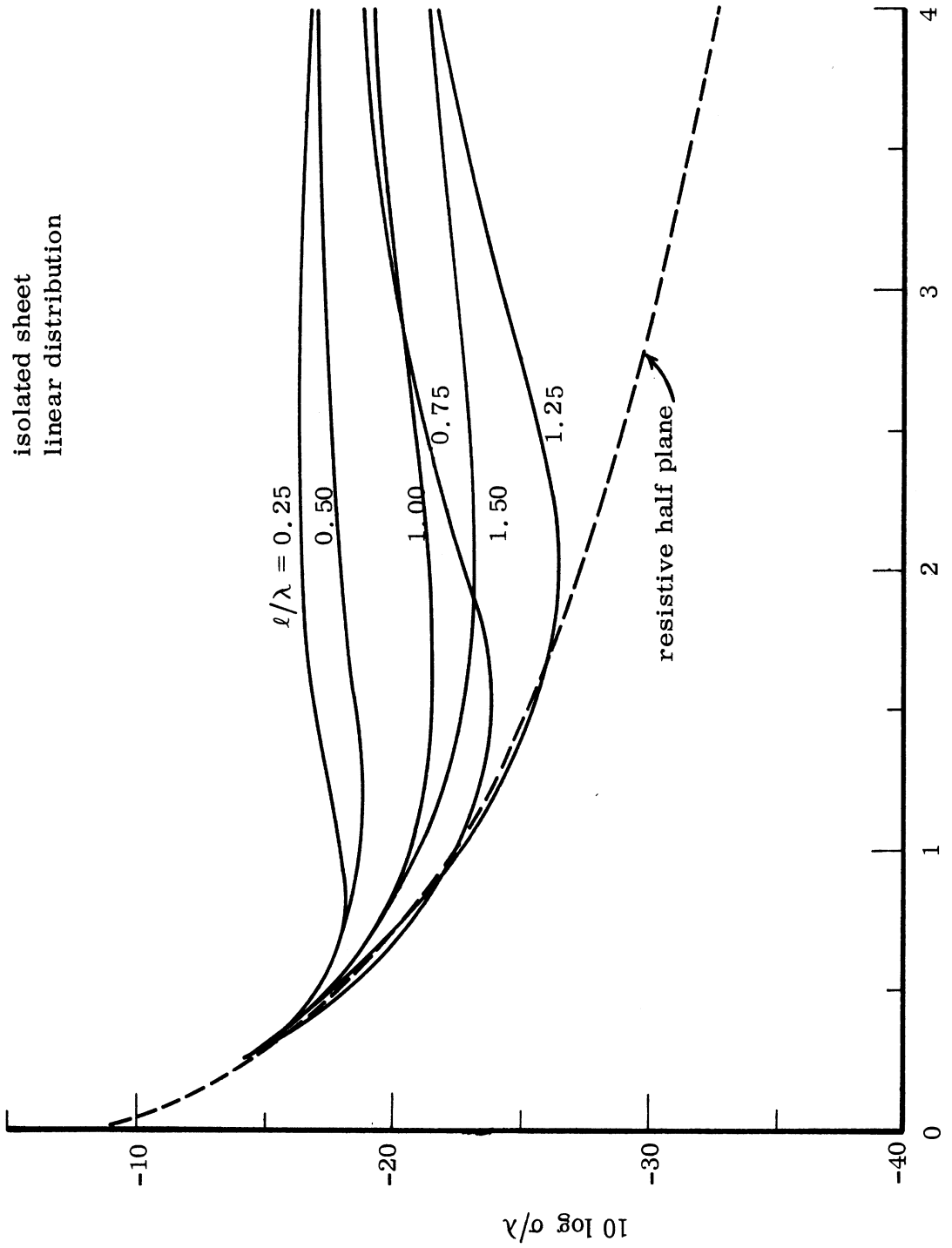

FIG. 7: Edge-on scattering from isolated sheet, linear resistance distribution.

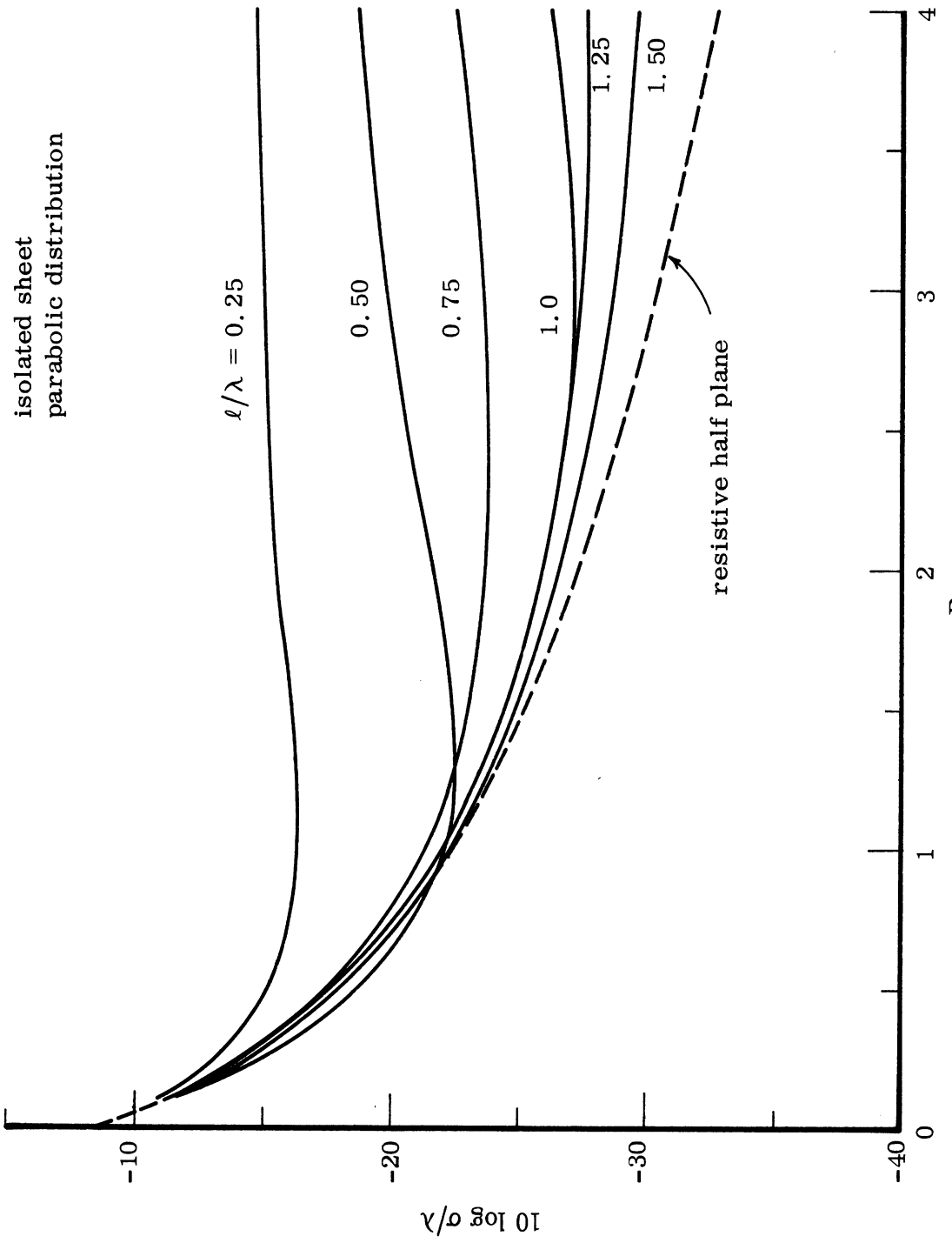

FIG. 8: Edge-on scattered from isolated sheet, parabolic resistance distribution.

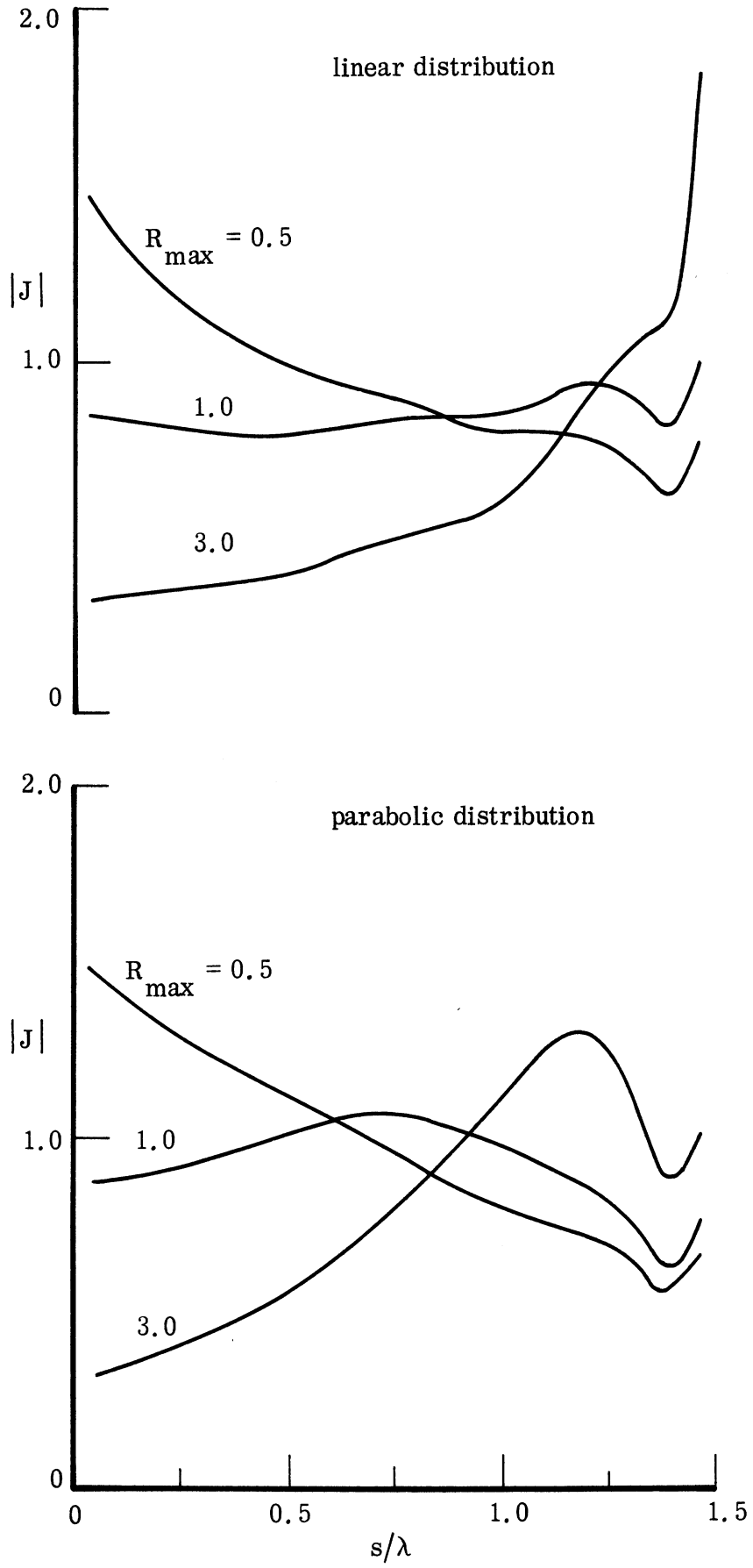

FIG. 9: Surface current distribution over isolated sheets for two resistance variations.

than in its presence. This deduction is consistent with the enhanced cross section levels noted in Figs. 7 and 8. Unfortunately, the isolated sheet results did not materially advance our understanding of Figs. 3 through 5.

V. The resistive half-plane

At about this time, because the leading edge sheet currents appeared to depend only upon R_{max}, it occurred to us that perhaps a resistive half-plane could be used to model the scattering from the leading edge of a finite sheet, even though the resistivity of the half plane must be constant in order to be theoretically treatable. As noted by Knott and Senior (1973), a resistive sheet is equivalent to an impedance boundary condition sheet provided we make the identification

$$\eta = 2R/Z_o \quad ,$$

where η is the normalized half plane impedance and R is the surface resistance at the edge of the sheet. Thus the diffraction coefficient of a resistive sheet can be obtained from the exact analytical solution for a constant impedance half plane, and for edge-on incidence this coefficient is applicable for all bistatic angles. On the basis of this identification, the edge-on cross section of a resistive sheet is plotted in Fig. 10 as a function of the edge resistance and the resulting curve is the basis for the dashed reference lines referred to in earlier figures. If the total scattering from a cylinder-sheet configuration is dominated by the leading edge alone, Fig. 10 suggests that a normalized edge resistance of about 7.0 is required for a cross section reduction of 30 dB.

VI. Deducing the junction contribution

Since the resistance half plane seemed to describe the net scattering quite well for sheets having parabolic and cubic resistance distributions, as judged by the dashed lines in Figs. 4 and 5, at least for sheet widths ℓ greater than (about) 0.5λ, we sought to use this information to extract the contribution of the junction

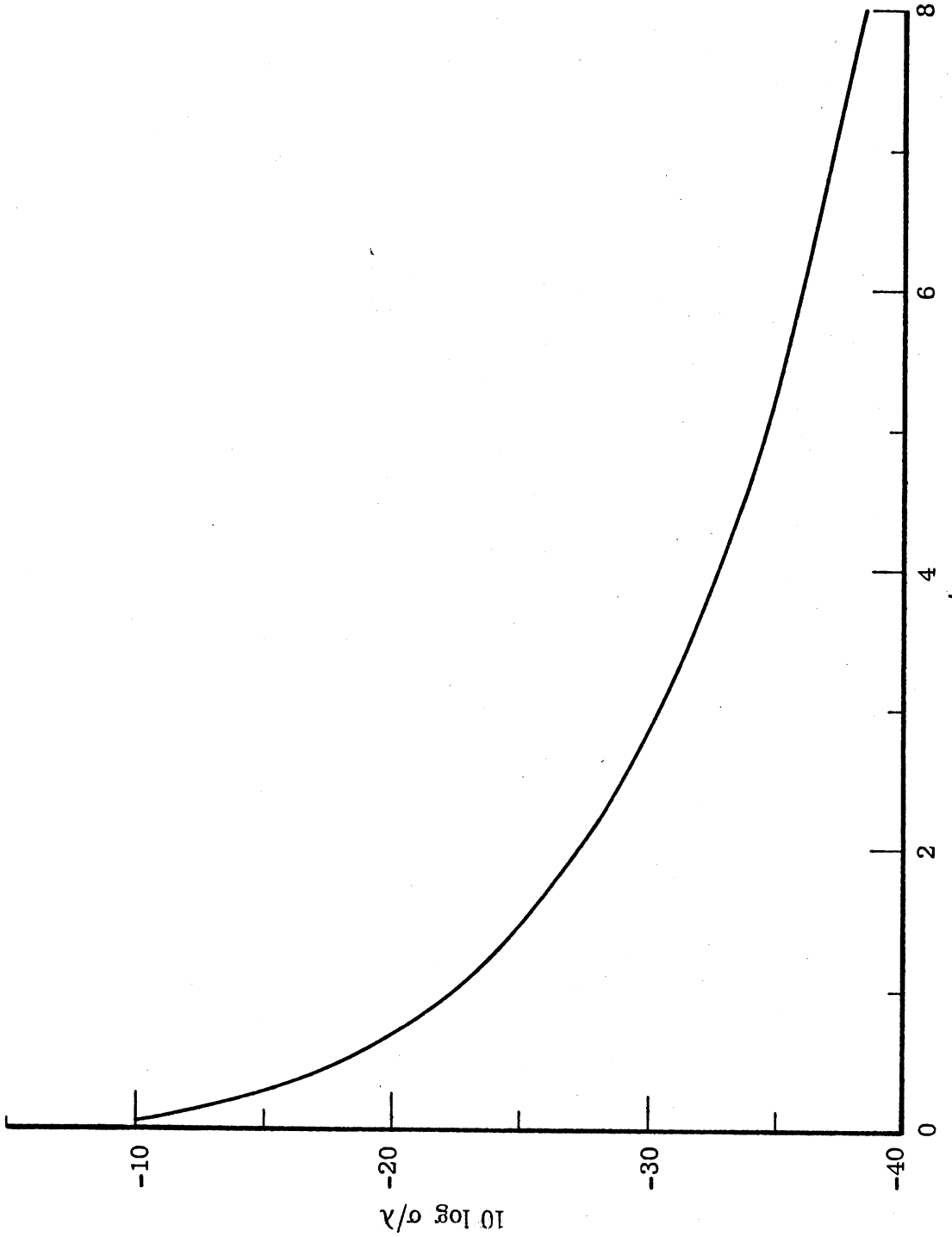

FIG. 10: Edge-on cross section of resistive half-plane of resistance R.

where the trailing edge of the sheet joins the leading edge of the cylinder. However, since program REST printed only amplitude data, a modified version was constructed (program RISK) so that phase was also provided on output. The decomposition of the total scattering into its component parts proceeds as follows: represent the scattering from leading edge as P_ℓ, that from the junction as P_j, and ignore the trailing edge return from the metallic cylinder. The net scattering is then

$$P = P_\ell e^{-i2k\ell} + P_j \quad ,$$

where ℓ is the distance between the two edges (i.e., the sheet width). It is convenient to normalize the two contributions with respect to the diffraction from an infinite metallic half plane, for which $P_o = -i/2$. If we let

$$A = P_\ell/P_o, \quad B = P_j/P_o \quad ,$$

then

$$P/P_o = B + A e^{-i2k\ell} \quad .$$

The left side is directly obtainable from the output of program RISK and since A is known from the impedance half plane solution, we may easily find B, the normalized junction contribution. The deduced junction return is plotted for linear, parabolic and cubic distributions in Figs. 11 through 13, and it is quickly seen that, except for the narrowest sheets (0.25λ and 0.5λ), it is much larger for the linear distribution than for either the parabolic and cubic distributions. Moreover, although we do not display the data, the phase of B for the linear case is essentially constant and independent of the leading edge resistance as well as the sheet width.

The linear case (Fig. 11) exhibits a distinct pattern not readily discernible in the other two cases: for a given leading edge resistance R_{max}, the junction return seems to increase as the sheet width increases. Suspecting that it was

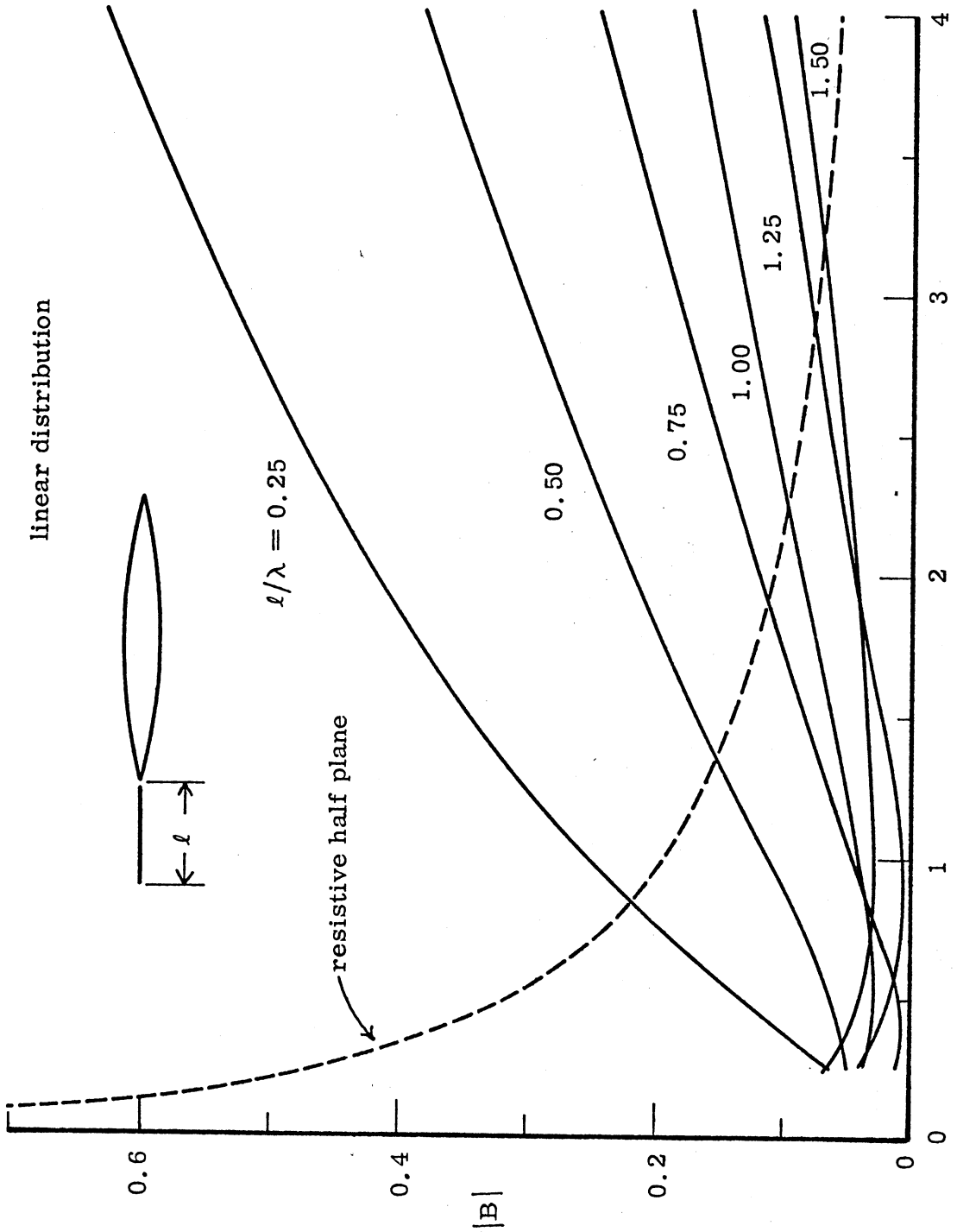

FIG. 11: Junction return for linear resistance distribution.

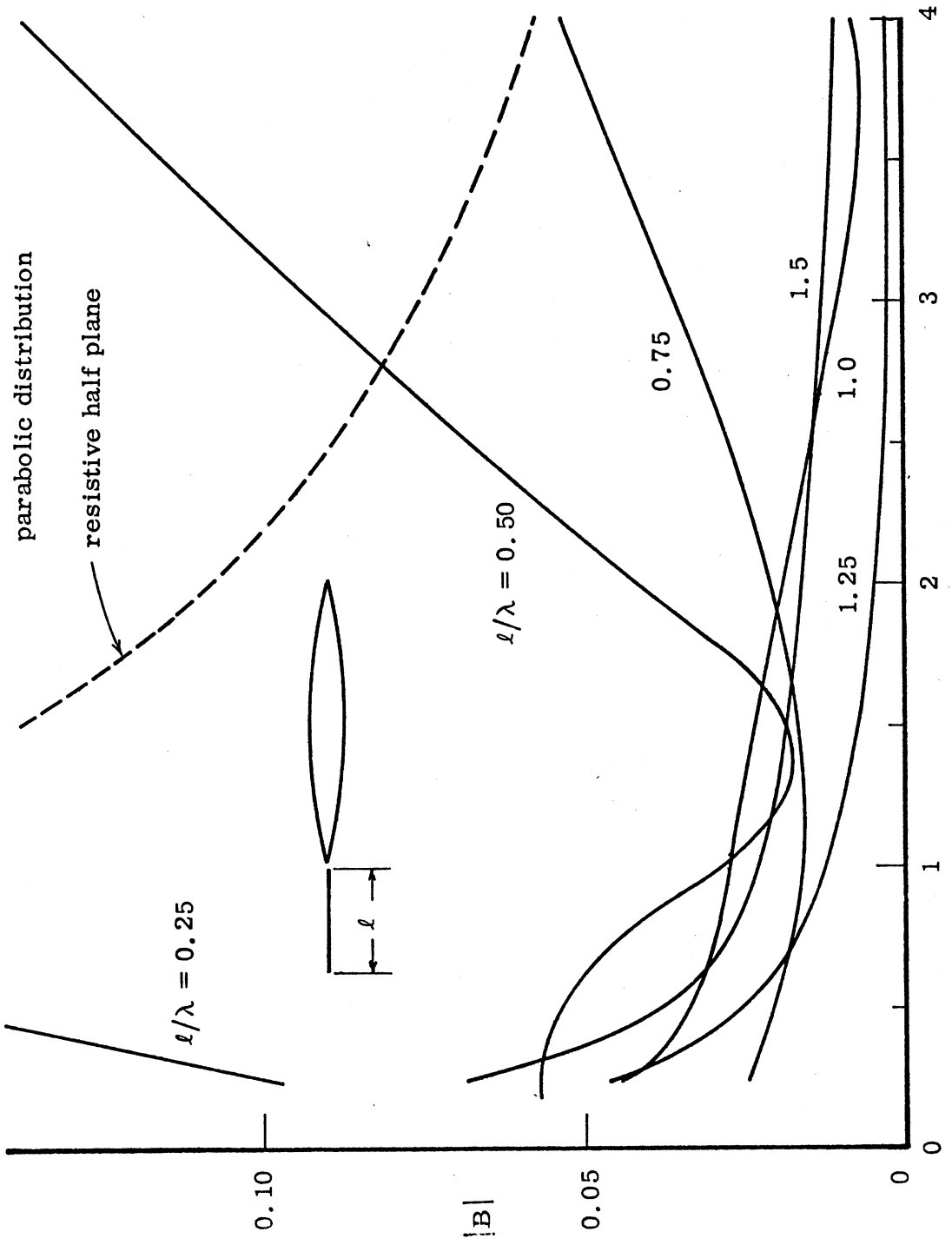

FIG. 12: Junction return for parabolic resistance distribution.

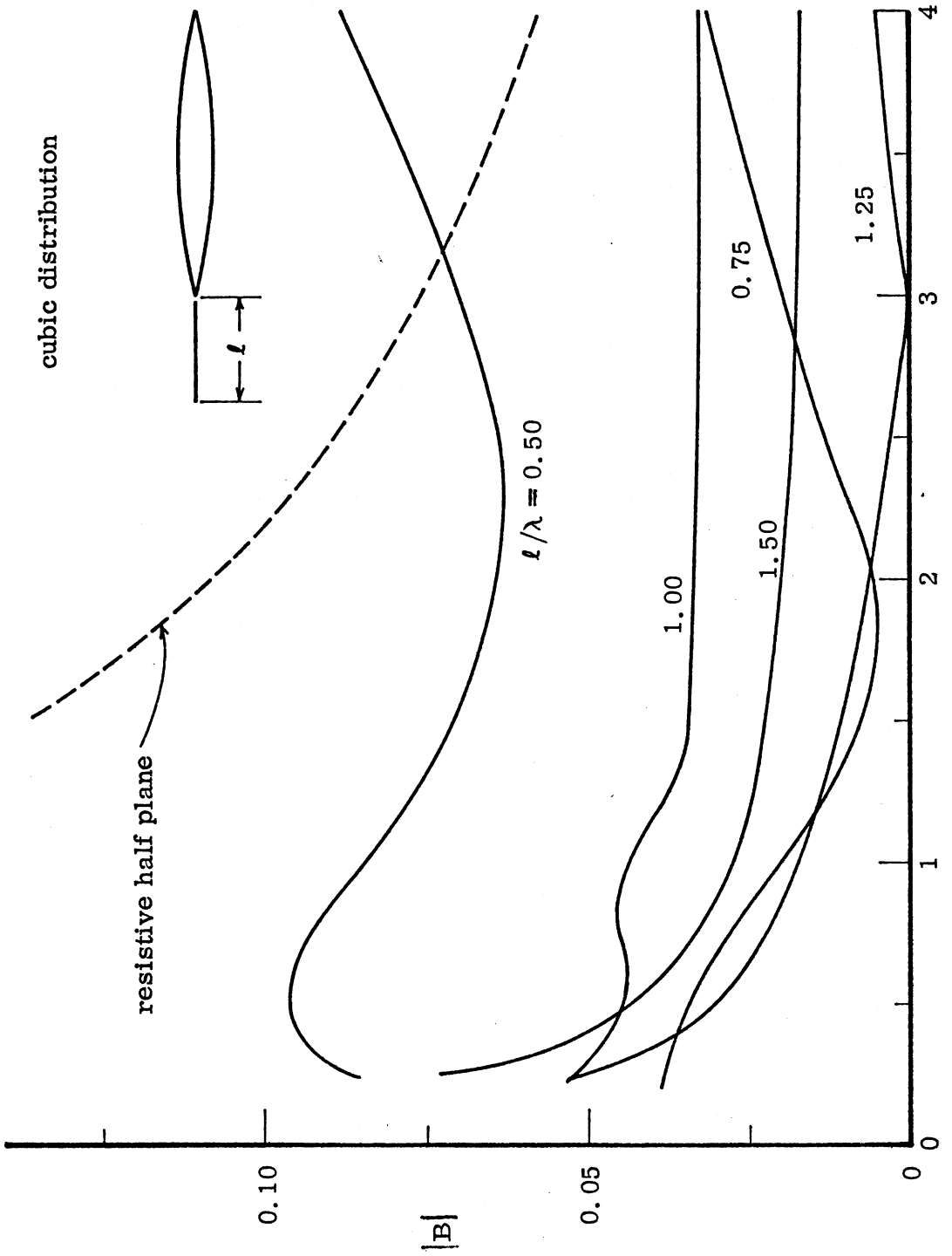

FIG. 13: Junction return for cubic resistance distribution.

the discontinuity in the slope of the resistance distribution at the rear edge of the sheet that produced the return there, we replotted the data as in Fig. 14 as a function of R_{max}/ℓ, instead of R_{max}. Note that although there is a dispersion in the data depending on the precise width of the sheet, the rate of increase of the junction return is essentially independent of the sheet width and is given approximately by

$$|B| = 0.048 \frac{R_{max}}{\ell} .$$

Thus the scattering from the junction is directly proportional to the slope of the resistance curve there.

By way of verifying this concept, we carried out another numerical experiment using an exponential variation of the form

$$R = R_{max} e^{-mx} ,$$

where x is the distance rearward from the leading edge. The sheet width was fixed at 1λ and the slope of the resistance curve depends upon both R_{max} and the constant m in the exponent. Nine discrete values for m were chosen, ranging from about 0.1 to 0.9. As outlined above, the amplitude of the junction contribution was extracted and the results are plotted in Fig. 15 as a function of the slope at the rear edge. The deduced value of the dependence on slope is

$$|B| = 0.045 \tan\delta ,$$

and is quite close to that obtained using the linear distribution.

Thus there appears to be no question that the slope of the resistance curve should be small or zero at the junction between the rear edge of the resistive sheet and the leading edge of the ogival cylinder. That this is true is borne out by the results for the parabolic and cubic resistance distributions, whose junction contributions tend to be nearly a magnitude smaller than that of the linear distribution. In fact, the deduced junction returns plotted in Figs. 12

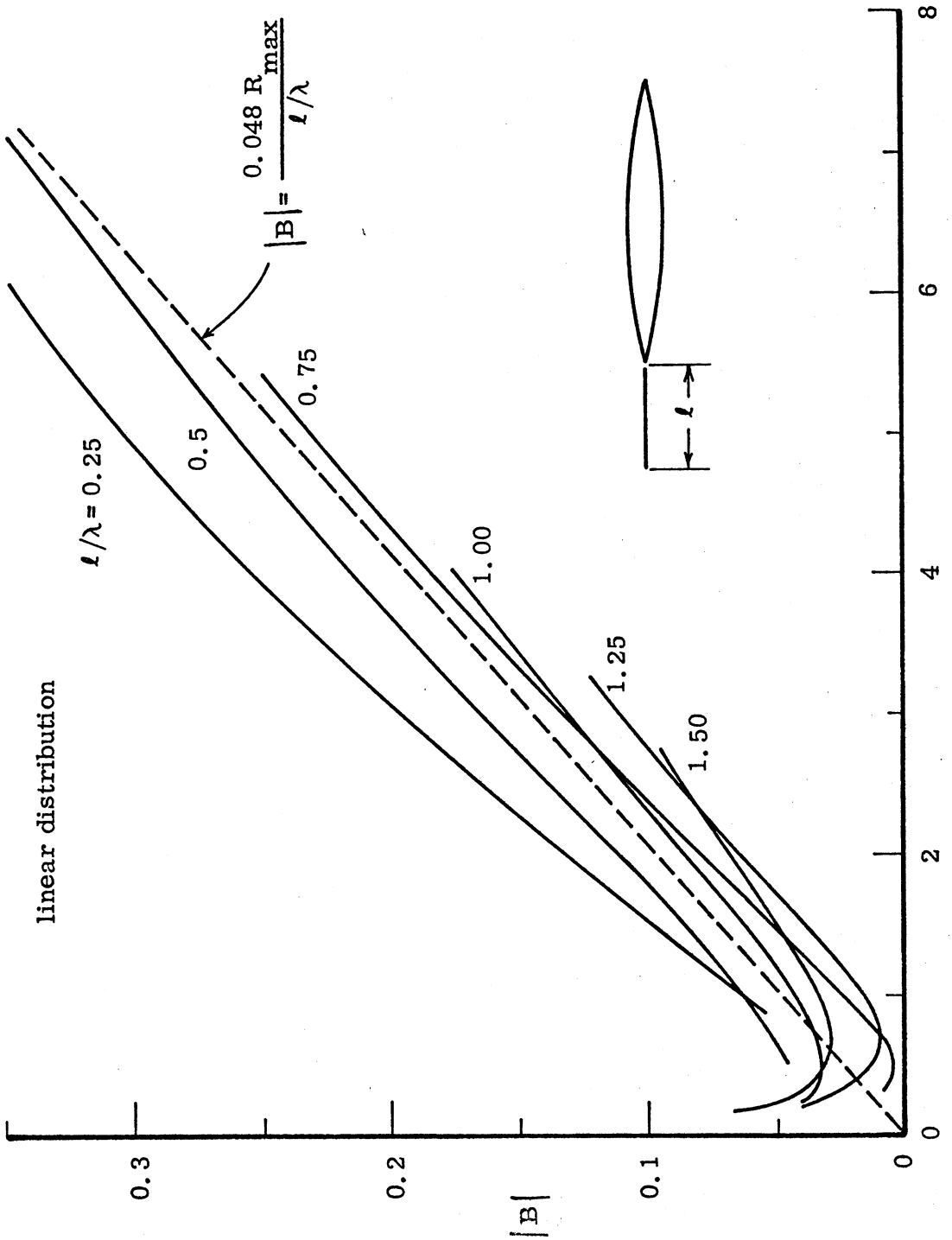

FIG. 14: Junction return for linear resistance distribution as a function of slope.

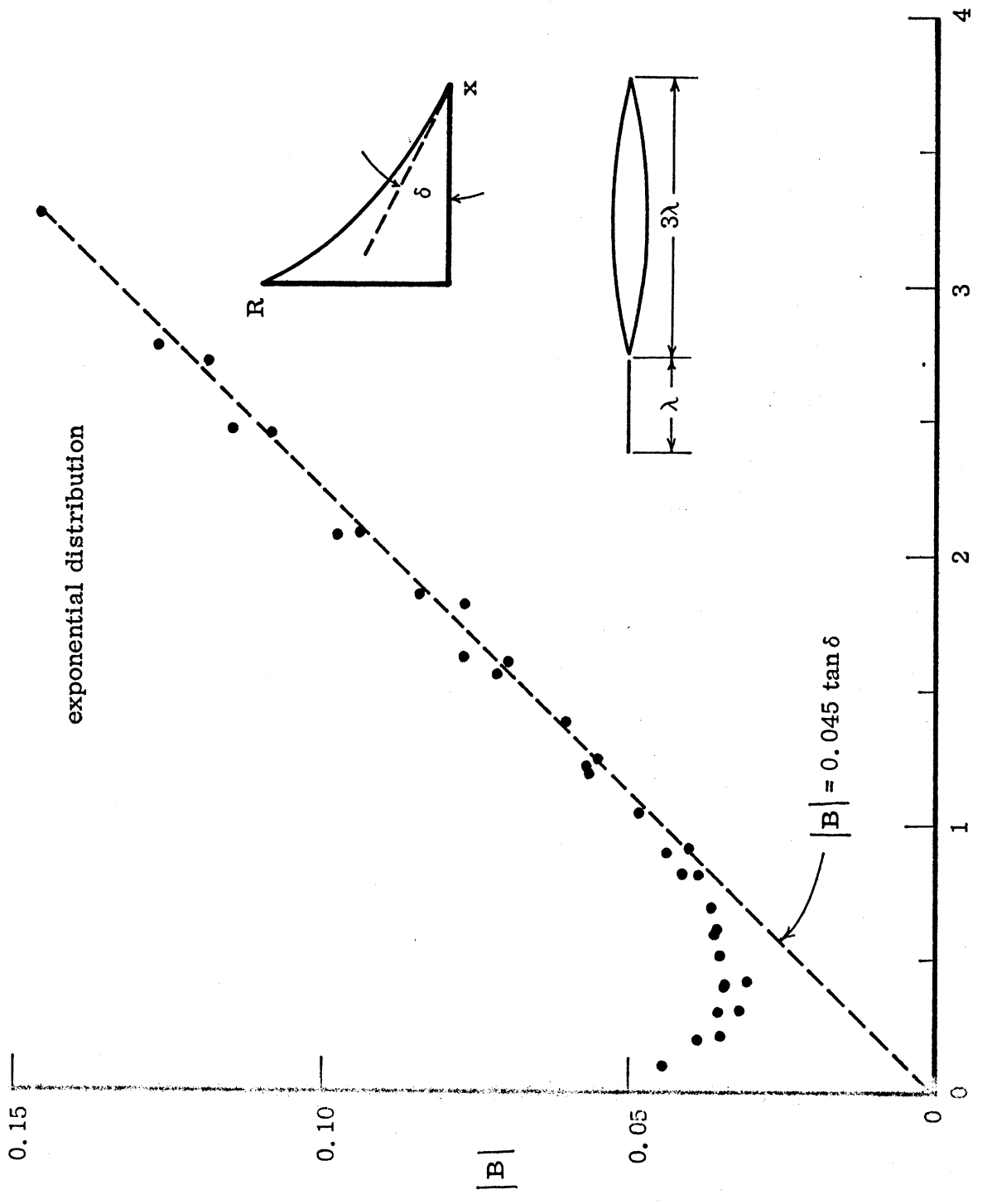

FIG. 15: Junction return for exponential resistance distribution as a function of slope.

and 13 are probably contaminated by errors because they were obtained from the phasor difference between a pair of comparable complex numbers, one a "measured" value via program RISK and the other the theoretical value for A, the resistive half plane scattering. We have not yet tried to determine the influential parameters for the behavior seen in Figs. 12 and 13, primarily because no distinct pattern like that in Fig. 11 suggests itself. It is also possible that the trailing edge return of the metallic cylinder must now be included in the decomposition process because the cross section levels are low enough that the small (but finite) rear edge return is no longer negligible.

VII. Conclusions

It is clear that linear distributions should be avoided because of the danger of creating a discontinuity in slope at the trailing edge of the resistive sheet. Theoretically, a distribution of the form $(\ell - x)^n$ has zero slope at the trailing edge (provided $n > 1$), so that $(\ell - x)^{1.005}$, for example, could be an acceptable distribution. However, a numerical implementation never approaches this condition because of the finite sampling required, hence n should be chosen to be substantially different than unity. We have studied only $n = 2$ and $n = 3$, and while these appear to be favorable in reducing the junction contribution, there remains the front edge return which can be made smaller only by choosing a high enough value of R_{max}.

Although Fig. 10 suggests that $R_{max} \simeq 7$ should reduce the cross section by 30 dB, it still will apparently require a sheet of at least 0.75λ wide in order to be useful. In the coming months we plan to test this hypothesis and to determine if such a large value of R_{max} can be used in conjunction with sheets of this width. In the meantime, since the resistive sheets are useful only for E-polarization, we plan to examine the use of magnetic resistive sheets for H-polarization by means of the expansion of program TWOD. As pointed out earlier, we hope to produce a generalized program incorporating electric and magnetic resistive sheets, and including a surface impedance boundary condition, for both E- and H-polarization.

References

Knott, E. F. and T. B. A. Senior, "Non-specular radar cross section study," Air Force Avionics Laboratory Technical Report AFAL-TR-73- , University of Michigan Radiation Laboratory Report No. 011764-1-T, November 1973.

Knott, E. F., V. V. Liepa and T. B. A. Senior, "Non-specular radar cross section study," Air Force Avionics Laboratory Report AFAL-TR-73-70, University of Michigan Radiation Laboratory Report No. 011062-1-F, April 1973.